Carbon nanotube filters

A. SRIVASTAVA[1], O. N. SRIVASTAVA[1]*, S. TALAPATRA[2], R. VAJTAI[2] AND P. M. AJAYAN[2]*

[1]Department of Physics, Banaras Hindu University, Varanasi, India-221005

[2]Department of Materials Science & Engineering, Rensselaer Polytechnic Institute, Troy, New York 12180-3590, USA

*e-mail: hepons@yahoo.com; ajayan@rpi.edu

Published online: 1 August 2004; doi:10.1038/nmat1192

Over the past decade of nanotube research[1], a variety of organized nanotube architectures have been fabricated using chemical vapour deposition[2–5]. The idea of using nanotube structures in separation technology has been proposed[6–8], but building macroscopic structures that have controlled geometric shapes, density and dimensions for specific applications still remains a challenge. Here we report the fabrication of freestanding monolithic uniform macroscopic hollow cylinders having radially aligned carbon nanotube walls, with diameters and lengths up to several centimetres. These cylindrical membranes are used as filters to demonstrate their utility in two important settings: the elimination of multiple components of heavy hydrocarbons from petroleum—a crucial step in post-distillation of crude oil—with a single-step filtering process, and the filtration of bacterial contaminants such as *Escherichia coli* or the nanometre-sized poliovirus (~25 nm) from water. These macro filters can be cleaned for repeated filtration through ultrasonication and autoclaving. The exceptional thermal and mechanical stability of nanotubes, and the high surface area, ease and cost-effective fabrication of the nanotube membranes may allow them to compete with ceramic- and polymer-based separation membranes used commercially.

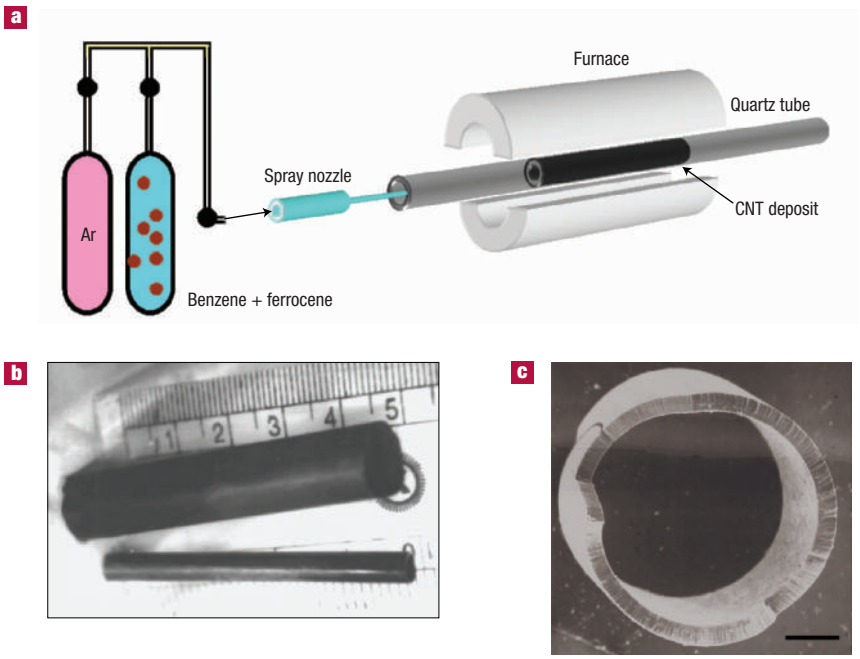

Figure 1 Production of the macro architecture of aligned nanotubes for use in filtration applications. a, Schematic of the spray pyrolysis set for growing aligned MWNTs. The process consists of a nozzle attached to a ferrocene/benzene solution supply used for releasing the solution into a quartz tube, mounted inside a temperature-controlled cylindrical furnace. Benzene/ferrocene solution was injected into the quartz tube, using argon as a carrier gas. The temperature of the furnace was raised to 900 °C. The formation of the CNT macrostructure was strongly dependent on the nozzle size and flow rate of the solution. The removal of the assembled bulk nanotube column was done by careful infiltration of acid along the inner wall of the quartz tube. **b**, Photograph of the bulk tube. **c**, SEM image of the aligned tubes with radial symmetry resulting in hollow cylindrical structure (scale 1 mm).

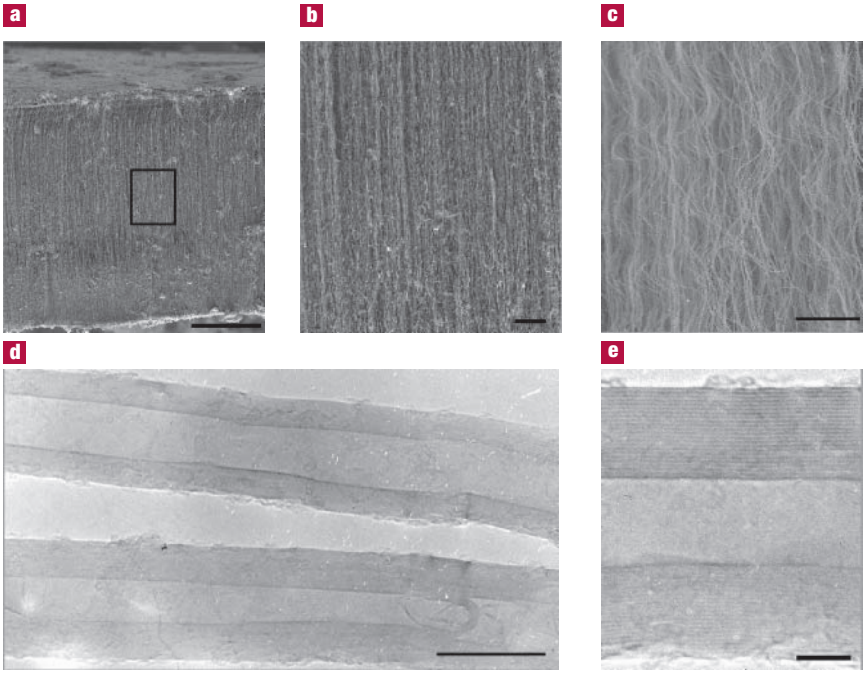

Figure 2 Structural characterization of macrotubes made from MWNTs. a, SEM image of the cylindrical macrostructure assembly showing the wall of the bulk tube consisting of aligned MWNTs with lengths equal to the wall thickness (scale 100 μm). A magnified view of the portion outlined by the rectangle is shown in **b**. **b**, SEM image of the dense packing of the nanotubes in the membrane (scale 10 μm). **c**, SEM image of a thin section extracted from the membrane, and subjected to a short oxidative etching (scale 5 μm). Some thinning of the nanotubes allows better visualization of the nanotube structure that make up the macrotube. **d**, TEM image of the tubes forming the macro structure (scale 20 nm). **e**, High-resolution TEM of a typical nanotube that forms the macrotube structure, showing well-graphitized walls of the MWNT (scale 5 nm).

The ability to fabricate robust membrane-like structures with carbon nanotubes (CNTs) can lead to a range of applications in separation technologies, particularly given the selective adsorption properties of nanotube surfaces[6–12]. In order to perform various separation applications with nanoscale structures in a practical way, appropriate large-scale structures need to be designed and built with nanoscale units. By using a continuous spray pyrolysis method (Fig. 1a) we have synthesized macroscale hollow carbon cylinders up to centimetres in diameter and several centimetres long, with walls (ranging from 300 μm to 500 μm thick) consisting of micrometre-length aligned multiwalled nanotubes (MWNTs). The aligned nanotubes that form uniform nanoporous, cylindrical membrane walls, are synthesized from sprayed ferrocene-derived iron catalyst particles; the nanotubes grow in radial directions on the walls of removable silica tube templates, leading to the formation of free-standing and continuous hollow cylindrical carbon tubes. Figure 1b,c provides the details of the monolithic nanotube macrotube formation.

Detailed structural characterization of the CNT macrotube is shown in Fig. 2. In Fig. 2a, a broken piece from a 300-μm-thick macrotube wall, consisting of well-aligned MWNT bundles is shown. The length of the MWNTs corresponds to the wall thickness of the bulk structure. Figure 2b shows the dense packing of these aligned structures. An scanning electron microscope (SEM) image of a thin section extracted from the membrane is shown in Fig. 2c. Figure 2d,e shows transmission electron microscopy (TEM) images of the tubes forming these macro structures. Figure 2e shows the high-resolution TEM image of a typical nanotube in the macrotube assembly, showing the well-graphitized walls of the MWNT. The range of inner and outer diameters of these nanotubes were found to be ~10–12 nm and ~20–40 nm respectively from TEM analysis. Volumetric adsorption isotherm measurement (using high-purity nitrogen gas as adsorbate) at 77.3 K was performed to estimate the specific surface area (SSA) offered by these structures. The SSA value obtained from the monolayer completion of the adsorbed nitrogen was found to ~50 $m^2 g^{-1}$, which is comparable to the SSA of typical MWNTs grown using a chemical vapour deposition process (A. D. Migone, private communication; detailed isotherm results will be presented elsewhere).

The macrotube is found to be mechanically very stable. The nanotube filters remained stable even after ultrasonic treatment showing the high mechanical stability of the assembled carbon architectures. We have performed direct tensile tests on various small pieces (~1–2 mm wide) of the assembled structure by applying a load parallel to the bulk tube axis. The values for the Young's modulus obtained from the true stress versus the true strain curves (see Supplementary Information for details) was ~50 MPa and the tensile strength was ~2.2 MPa (comparable to other assembled graphitic materials[13]). Three-point bend tests on these bulk structures were performed to quantify the breaking strength of the macro tubes. The fracture load (at the weakest point) of the tube was found to be ~2 N (details of the experiments are presented in the Supplementary Information). Failure-to-pressure tests for the bulk tube were conducted by sealing the tube (in a similar arrangement and using the same cell that was used in petroleum filtration process, discussed later in the text) on one end and then evacuating it to 0.01 mbar. The decrement in vacuum inside the bulk tube was dynamically monitored with time. Initially (within 60 s) the pressure inside the tube increased rapidly to ~0.5 mbar and then slowly (~200 s) equilibrium was achieved at 0.6 mbar pressure. The time versus inner tube pressure data (see Supplementary Information) shows that these bulk structures were capable of sustaining a considerable amount of pressure difference (inner wall ~10^{-2} mbar and outer wall 1 atm.) and

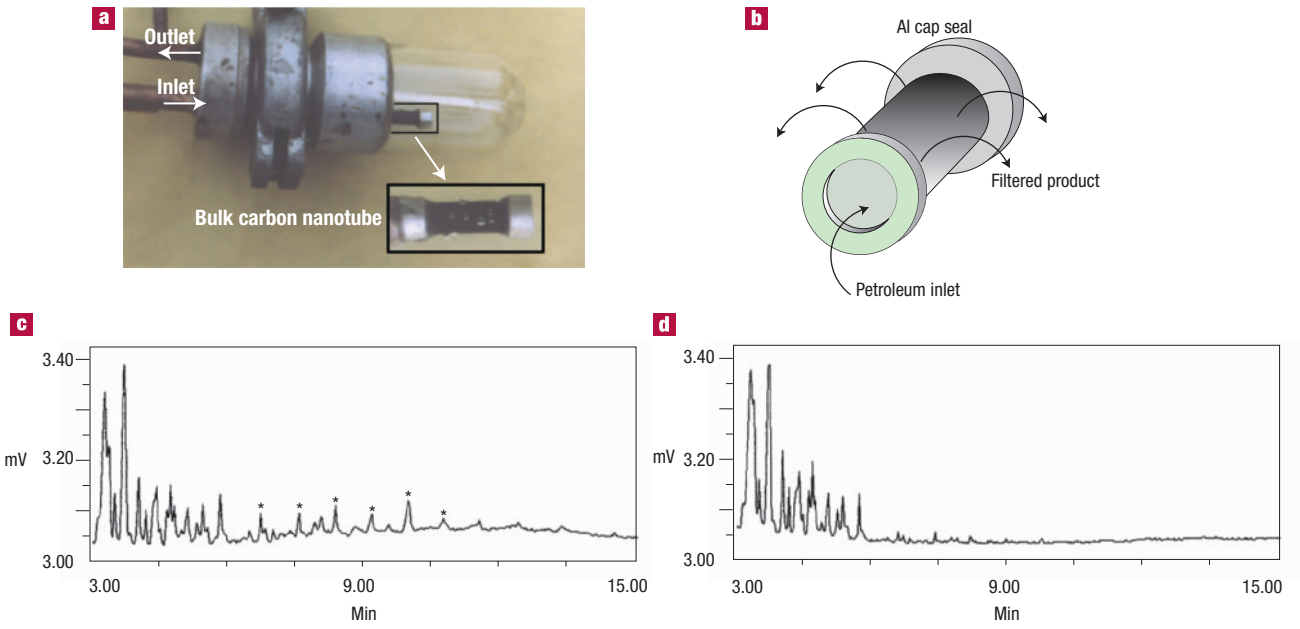

Figure 3 Petroleum filtration set-up using the nanotube filter. a, Photograph of the arrangement used for heavy hydrocarbon separation. The inset shows the bulk tube mounted as a filter. The tube is closed at one end (right) with an aluminium cap, and the other end is kept open serving as an inlet port for injection of petroleum. **b**, Schematics of the petroleum dynamics through the bulk tubes. **c**, GC spectrum of the unfiltered products. The asterisks show the heavier hydrocarbon components in the unfiltered sample. **d**, GC spectrum of the sample after it was passed through the nanotube filter, showing the absence of heavier hydrocarbon peaks. The sample to be separated was introduced into a fused silica capillary column, having a length of 10 m and inner diameter of 530 μm, through an injection port and was swept down the column by nitrogen. The loop volume used for injection was 50 μl. The temperature of the column was controlled in such a way that the substances being separated had a suitable vapour pressure and could move through the column at a rate proportional to their respective vapour pressures. The temperature of the column was set at 50 °C for two minutes and thereafter was raised to 240 °C at a rate of 20 °C per minute. The detector temperature was fixed at 260 °C.

hence suggests the robustness of these solid carbon filters. The ability of the bulk tube to maintain a constant pressure difference also suggests that these structures are devoid of any cracks or surface defects.

The potential use of the nanotube-based macrostructure was explored in the filtration of heavier hydrocarbon species, C_mH_n ($m>12$), from hydrocarboneus oil for example, petroleum C_mH_n ($n = 2m + 2$, $m = 1$ to 12), and in the removal of bacteria from drinking water and filtration of the nanometre-sized poliovirus. Breaking large hydrocarbons into smaller ones or separating heavier hydrocarbons from crude oil is an important step in gasoline production and improvement of octane quality[14]. Octane number, which depends on the type of hydrocarbon present, also determines the antiknock ability of a fuel[15]. We have efficiently carried out the filtration of petroleum (C_mH_n) by separating multiple components of heavier hydrocarbons from it using these bulk nanotube-based tubes as filters. Figure 3a,b shows a representation of the separation process. Before filtration, the bulk nanotube filters were subjected to acid treatment for removal of metal impurities followed by ultrasonic cleaning on immersion in acid mixtures. The nanotube filter was mounted to the filtration set-up as shown in Fig. 3a (see figure caption for the geometry of the set-up and process details). The presence of various peaks in the spectrum represents specific C_mH_n components of petroleum. Filtered as well as unfiltered samples of petroleum were analysed by standard gas chromatography (GC; Nucon-5800C and Varian-1800) and flame-ionization detection techniques. Figure 3c,d shows the representative spectra of the petroleum sample before and after passing through the nanotube filter, respectively. The several peaks present in both the spectra shows the presence of C_mH_n components in petroleum. The presence of heavier hydrocarbon components in the unfiltered samples gives rise to the sharp peaks (marked by asterisks in the spectrum). The successful elimination of heavier hydrocarbons by the nanotube filter is seen in the spectrum obtained for the filtered sample. The elimination of the heavier hydrocarbons using the bulk tube filter was performed several times with reproducible results. It was also noted that these filters were able to eliminate various other cyclic compounds in contrast to linear C–H compounds (both of these have higher retention times than the spectrum shown in Fig. 3c,d). Detailed experimental conditions and spectra regarding the filtering of these compounds are presented in the Supplementary Information. A much simpler filtration process (separation of a mixture of naphthalene and benzene), was also carried out in order to demonstrate selectivity of these free-standing membranes (see Supplementary Information for the GC spectrum of unfiltered and filtered samples). The separation coefficient ($\alpha = 7.5$ for the just-filtered sample and 6 and 5.8 for the samples filtered after 10 and 20 minutes respectively) determined from the relative peak areas of the GC spectrum indicate that naphthalene is adsorbed in first few minutes and saturates in ~10 minutes.

Further use of the nanotube filters was evaluated for the successful removal of bacterial contamination from drinking water. A common pollutant of drinking water is the faecal bacterium *Escherichia coli* having a typical length of 2,000 nm to 5,000 nm and width 400 to 600 nm. This is responsible for many waterborne diseases. Our studies show that the nanotube filters we have fabricated could be used successfully to obtain bacteria-free water for human consumption[16]. Sterile saline water with light bacterial suspension (~10^6 organisms per ml) was analysed. The suspension has a light pink and turbid (Fig. 4a) colour, due to the fact that the bacteria colonies were scraped from the surface of MacConey agar, which contains Phenol red as an indicator.

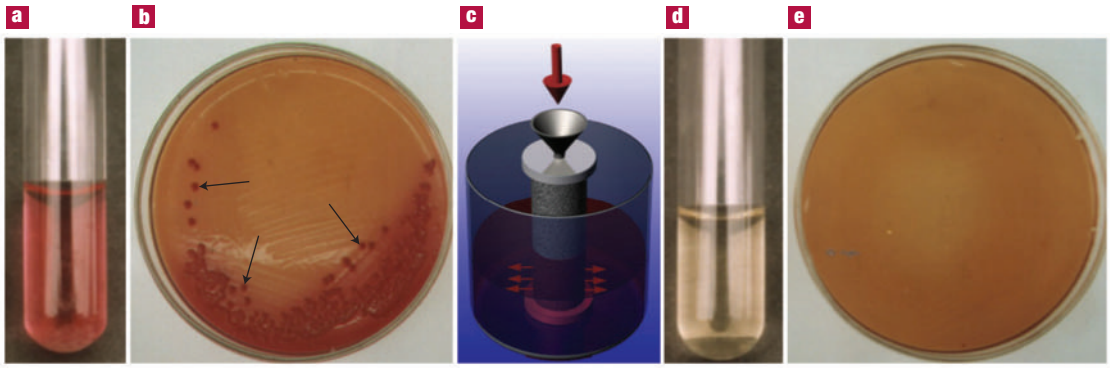

Figure 4 Removal of bacteria using nanotube filter. a, The unfiltered water containing *E. coli* bacteria; the turbid and light-pink colour is suggestive of the presence of bacteria colonies scraped from the surface of MacConey agar which contains Phenol red as an indicator. **b**, The colonies of *E. coli* bacteria (marked by arrows) grown by the culture of the polluted water. **c**, The assembly for the filtration experiment. The nanotube filter with the bottom end-capped was placed inside a container and the liquid was flowed through the macrotube (shown by the vertical arrow). The horizontal arrows show the flow direction of the filtered liquid. **d**, Shows the water filtered through nanotube macrofilter. The product obtained is relatively clear compared with the original bacterial suspension in **a**, indicating the absence of the bacteria (as well as colouring particles) in the filtrate. **e**, The filtrate after culture showing the absence of the bacterial colonies.

This bacterial suspension was subjected to a filtration process through the nanotube filters placed in a geometry similar to that used for end-flow geometry (Fig. 4c). The product of the filtration process is shown in Fig. 4d. The filtered fluid is pure saline water and does not have a pink turbid colour suggesting that after filtration *E. coli* bacteria have been eliminated. To confirm this and to check the efficiency of the filtration process, both the filtrate and the unfiltered bacterial suspension were cultured in solid as well as liquid media, and incubated at ~37 °C overnight. The unfiltered solution showed the growth of bacterial colonies (Fig. 4b indicated by arrows), whereas this growth was absent in the filtered product (Fig. 4e). Similar successful filtration was also achieved for another bacterium, *Staphylococcus aureus*, with a spherical size of 1,000 nm, smaller than *E. coli*. Similar to the case of water with *E. coli* bacteria, it was possible to remove the *S. aureus* bacteria entirely from water through filtration by the present nanotube filters. This efficient bio-adsorptive property of the filters was also tested for much smaller (nanoscale dimensions) species: polio-1 (poliovirus sabin 1, of sizes ~25 to 30 nm with a molecular mass of 8.5×10^6 daltons, and having icosahedral shapes)[17–19]. We were able to filter this nanometre-size poliovirus successfully using our macrotube–nanotube filters (see Supplementary Information for details of the experiment and the results). All the filtration processes were repeated several times with completely reproducible results.

We have observed steady flow rates during the experiments for a significant amount of time. Using the area of the membrane tube (5.55 cm^2) the flow rates were found to be 1.8 ml min^{-1} cm^2 for petroleum, 1.1 ml min^{-1} cm^2 for contaminated water and 2.2 ml min^{-1} cm^2 for the benzene and naphthalene mixture. The typical pressure difference was $\sim 8.8 \times 10^3$ Pa. The filtration process itself was driven by gravity as no additional pressure was applied. We believe that the confined geometry of the nanotubes (and hence nanoporosity) and the selective adsorption behaviour of the nanotube surfaces are both useful in the filtration process. Because the inter-tubular spaces dominate the porosity in the membrane, and as many of the nanotube's internal spaces possibly have plugs of metal particles, we believe that most of the filtering occurs in the interstitial spaces. We certainly cannot discount the fact that there might be some transport through the inner hollow channels of the tubes, but the exact distribution of these two mechanisms is very difficult to quantify. One concern in all the above-mentioned filtering processes is fouling. However, the uniform dense packing of the nanotubes in the radial direction of the solid macrotube filter provides an ideal geometry for cross-flow filtration favouring minimum blockage, and is effective for cleaning the filters with purging cycles.

A major advantage of using the nanotube filters over conventional membrane filters lies in the fact that they can be cleaned repeatedly after each filtration process to regain their full filtering efficiency. A simple process of ultrasonication and autoclaving (~121 °C for 30 mins) was found to be sufficient for cleaning these filters; cleaning can also be achieved by purging for the reuse of these filters. In conventional cellulose nitrate/acetate membrane filters used in water filtration, however, strong bacterial adsorption on the membrane surface affects their physical properties preventing their reusability as efficient filters[20]; most of the typical filters used for virus filtration (see, for example, ref. 21) are not reusable. Because of the high thermal stability of the nanotubes our filters can also be operated at temperatures of ~400 °C, which are several times higher than the highest operating temperatures of the conventional polymer membrane filters (~52 °C). The nanotube filters, owing to their high mechanical and thermal stability, may compete with commercially available ceramic filters; furthermore, in the future, these filters may be tailored to specific needs by controlling the nanotube density in the walls and the surface character by chemical functionalization.

Received 8 February 2004; accepted 29 June 2004; published 1 August 2004

References

1 Dresselhaus, M. S., Dresselhaus G. & Avouris, P. *Carbon Nanotubes: Synthesis, Structure, Properties and Applications* (Topics in Applied Physics Series, Springer, Heidelberg, 2001).
2. Li, W. Z. *et al.* Large scale synthesis of aligned carbon nanotubes. *Science* **274,** 1701–1703 (1996).
3. Ren, Z. F. *et al.* Synthesis of large arrays of well-aligned carbon nanotubes on glass. *Science* **282,** 1105–1107 (1998).
4. Huang, S. M., Dai, L. M. & Mau, A. W. H. Controlled fabrication of large-scale aligned carbon nanofiber/nanotube patterns by photolithography. *Adv. Mater.* **14,** 1140–1143 (2002).
5. Wei, B. Q. *et al.* Organized assembly of carbon nanotubes. *Nature* **416,** 495–496 (2002).
6. Hinds, B. J. *et al.* Aligned multiwalled carbon nanotube membranes. *Science* **303,** 62–65 (2004).
7. Casavant, M. J., Walters, D. A., Schmidt, J. J. & Smalley R. E. Neat macroscopic membranes of aligned carbon nanotubes. *J. Appl. Phys.* **93,** 2153–2156 (2003).
8. Miller, S. A., Young, V. Y. & Martin, C. R. Electroosmotic flow in template-prepared carbon nanotube membranes. *J. Am. Chem. Soc.* **123,** 12335–12342 (2001).
9. Long, R. Q. & Yang, R. T. Carbon nanotubes as superior sorbent for dioxin removal. *J. Am. Chem. Soc.* **123,** 2058–2059 (2001).
10. Yan-Hui, L. *et al.* Adsorption of fluorine from water by aligned carbon nanotubes. *Mater. Res. Soc. Bull.* **38,** 469–476 (2003).
11. Kalra, A., Hummer, G. & Garde, S. Methane partitioning and transport in hydrated carbon nanotubes. *J. Phys. Chem. B.* **108,** 544–549 (2004).

12. Skoulidas, A. I., Ackerman, D. M., Johnson, J. K. & Sholl, D. S. Rapid transport of gases in carbon nanotubes. *Phys. Rev. Lett.* **89,** 185901 (2002).
13. Kyotani, T., Mori T. & Tomoita, A. Formation of flexible graphite film from poly (acrylonitrile) using layered clay film as template. *Chem. Mater.* **6,** 2138–2142 (1994).
14. Stikkers, D. E. Octane and the environment. *Sci. Total Environ.* **299,** 37–56 (2002).
15. Albahri, T. A., Riazi, M. R. & Alqattan, A. A. Analysis of quality of petroleum fuels. *Energ. Fuel.* **17,** 689–693 (2003).
16. Collee, J. G., Fraser, A. G., Marimion, B. P. & Simmons, A. *Mackie and McCartney Practical Medical Microbiology* (Churchill Livingston, New York, 1996).
17. Putnak, J. R. & Phillips, B. A. Picormaviral structure and assembly, *Microbiol. Rev.* **45,** 287–315 (1981).
18. Phillips, B. A. In vitro assembly of polio-virus. II Evidence of the self-assembly of 14S particles into empty capsids. *Virology* **44,** 307–316 (1971).
19. Hogle, J. M., Chow, M. & Filman, D. J. Three-dimensional structure of polio virus at 2.9A resolution. *Science* **229,** 1358–1565 (1985).
20. Chwickshank, R., Duguid, N. P., Marmion B. P. & Swain, R. H. A. *Medical Microbiology* (Churchill, London, 1975).
21. http://www.millipore.com/publications.nsf/docs/DS1180EN00

Acknowledgements

This work was partly funded by the Ministry of Non-Conventional Energy Sources and the Department of Science and Technology (New Delhi). A.S. acknowledges a fellowship from the Council of Scientific and Industrial Research. We are thankful to A. S. K. Sinha, A. K. Gulati, P. Ramachandra Rao and G. Nath of Banaras Hindu University, Varanasi, India for providing facilities, help and discussions. We thank A. D. Migone for sharing the results of adsorption measurements prior to publication, A. Cao and Ray Dove for help with the TEM images and Donald R. VanSteele for help with the mechanical strength characterizations. S. T., P. M. A. and R. V. acknowledge funding support from the Rensselaer Polytechnic Institute, National Science Foundation, Nanoscale Science and Engineering Center and Philip Morris USA.
Correspondence and requests for materials should be addressed to O.N.S. and P.M.A.
Supplementary Information accompanies the paper on www.nature.com/naturematerials

Competing financial interests

The authors declare that they have no competing financial interests.